ELSEVIER

Polymer 43 (2002) 1365–1373

polymer

www.elsevier.com/locate/polymer

Glass transition and exclusion model in crystallization of polyether–polyester block copolymers with amide linkages

Rong-Ming Ho*, Chih-Wei Chi, Chi-Chun Tsai, Jiang-Jen Lin

Department of Chemical Engineering, National Chung Hsing University, Taichung 40227, Taiwan, ROC

Received 2 July 2001; received in revised form 24 September 2001; accepted 26 September 2001

Abstract

Polyether–polyester block copolymers having various polyetheramide contents were synthesized. Single glass transition intermediated in temperature between the glass transition temperatures of polyester and polyetheramide components was found for all of polyether–polyesters. The compositional variation of glass transition exhibited a similar trend to the predicted result of thermodynamic theory for compatible polymer blends. The incompatible pair of homopolyester and homopolyether was forced to be compatible after copolymerization. A modified theoretical prediction for the glass transition of copolymers based on the thermodynamic theory is proposed. Consistent results between theoretical prediction and experimental measurements were found. Unlike homopolyesters, the glass transition temperature of copolymer amorphous domains gradually decreases with crystallization time. An exclusion model for the crystallization of polyester segments in copolymers is proposed. The temperature width of the glass transition increases with crystallization time. The broadening towards the low temperature side in glass transition is interpreted as the evidence of crystallization-induced partial phase separation. Instead of forming macroscopic segregation, the excluded polyether segments resided in-between crystalline polyester lamellae and mix with amorphous polyesters to generate amorphous domains exhibiting concentration gradient along the lamellar basal surface normal. Further increasing the polyetheramide segment content brings the excluded polyetheramide segments to form domains among the crystallized polyester spherulites so as to inhibit the occurrence of spherulitic impingement.

Keywords: Exclusion model; Polyether–polyester; Crystallization

1. Introduction

The copolymerization of low molecular weight polyether, such as poly(ethyleneoxide) (PEO), with terephthalic polyesters to form segmented copolymers has been used to prepare thermoplastic elastomers (TPE) [1]. Polyether acts like a soft segment to provide rubber-like properties for the terephthalic polyester [2–14]. Polyether–polyesters have been identified to be semicrystalline-like materials, possessing crystalline polyester domains and well-mixed amorphous polyether and polyester domains [4–7,11]. More recently, the polyether–polyesters have drawn attention for their hydrophilic properties. A small amount of PEO (usually below 10 wt%) is introduced to PET by copolymerization in order to increase their hydrophilicity [15]. Crystallization kinetics of the low ether content polyether–polyesters has been analyzed via Avrami treatment combined with morphological observations by polarized light microscopy (PLM) and transmission electron microscopy (TEM). A crystallization mechanism through the heterogeneous nucleation process with homogeneous lamellar branching was proposed [16]. PEO homopolymer is also a crystallizable polymer. However, the crystallizability of PEO segments in polyether–polyesters is strongly affected by the molecular weight of PEO segment. At molecular weights below 4000 g mol^{-1}, PEO segments become non-crystallizable because of too short blockiness for crystallization. The crystallizability is thus restricted by the blocking effect of polyester segments [1]. In general, polyether–polyesters are prepared by copolymerization of ethylene glycol, dimethyl terephthalate (or terephthalic acid) and PEO having molecular weights ranging from 1000 to 4000 g mol^{-1}. A variety of copolymer properties can thus be tailored through the control of non-crystallizable PEO content.

In this study, a variety of polyether–polyesters with amide linkage has been synthesized. For terephthalic polyesters, there is always a problem about transesterification and/or degradation such as hydrolysis on polymer molecules after high temperature treatment. Furthermore,

* Corresponding author. Tel.: +886-4-2285-7471; fax: +884-4-2285-4734.

E-mail address: rmho@dragon.nchu.edu.tw (R.-M. Ho).

0032-3861/02/$ - see front matter
PII: S0032-3861(01)00680-2

the polyether is easy to cause degradation at higher temperature. Severe transesterification and/or degradation reaction may lead to a significant change in the thermal properties. In contrast to homopolyesters and homopolyether, the polyether–polyesters with amide linkages are found to be less susceptible to transesterification and degradation. This improvement is consistent with the literature reporting that the addition of phenolic antioxidants with amide linkages provides protection with preference to other phenolic antioxidants for polyester elastomers [17,18]. The amide linkages make the polyether–polyesters good candidate for thermal property measurements. We are interested in the compatibility of polyether and polyester segments at different compositions of copolymerization, particularly the compositional variation of glass transition temperature of the copolymers. The prediction of glass transition temperatures in compatible mixtures has been extensively studied before on the basis of the configurational entropy theory [19–21]. A modified theoretical prediction for the glass transition of copolymers based on the thermodynamic theory derived by Couchman and coworkers [20,21] is proposed and discussed in this study.

The studies of crystallizable copolymers, in particular those having diblock or triblock configurations, have been devoted to the changes on phase morphology after crystallization and the arrangement of chain folding with respect to microstructures [22–29]. Final morphology after crystallization depends on whether the sample is cooled from a microphase-separated melt or crystallizes from a homogeneous melt. The degree of segregation inevitably influences the final texture of crystallized copolymers. However, there have been few studies on the crystallization mechanism with respect to the action of constituted segments. In contrast to the studies of crystallized morphology for diblock or triblock copolymers, the studies on the morphology of crystallizing copolymer chain for segmented copolymeric materials are relatively absent. To explore the crystallization behavior of crystallizable segmented copolymers, the exclusion of polyetheramide segments in the progress of polyester crystallization was visualized by thermal analysis combined with morphological observations in this study.

2. Experimental section

2.1. Materials

Samples of polyether–polyesters with amide linkages were synthesized by copolymerization of terephthalic acid, ethylene glycol, and PEO diamine oligmer (Jeffamine® ED-2003, purchased from Huntsman Chemical), as previously described by Sheen and Lin [15]. To an autoclave, equipped with a heating device, temperature controller, vacuum pump and mechanical stirrer, were charged terephthalic acid, ethylene glycol, Jeffamine® ED-2003,

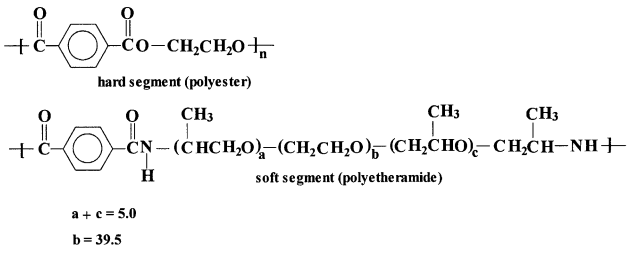

Fig. 1. Repeat unit structure of polyether–polyester copolymers.

GeO_2 and *p*-toluene sulfonic acid. While stirring, the mixture was slowly heated to 230 °C, held for 4 h, and then subjected to a vacuum gradually to reach 1 Torr pressure. During depressurization, the mixture was continuously heated to reach 260 °C, and then held for 2 h. The molecular weight of the PEO diamine was about 2000 g mol^{-1}. The repeat unit structure of the polyether–polyester copolymers prepared is shown in Fig. 1.

Different polyether–polyesters having soft segment content from 0 to 50 wt% were prepared and characterized. The composition of the copolymers was determined on the basis of the composition of reaction mixtures, as the composition has been identified to be in good agreement with the results from elemental analysis and NMR spectroscopy analysis [30,31]. For the purpose of systematic comparison, the reaction was monitored by the torque value of mixing during copolymerization in order to obtain the polyether–polyester with a close molecular weight. The intrinsic viscosity of the polyether–polyesters was measured in 1,1,2,2-tetrachloroethane at 30 °C using a capillary viscometer. The value of intrinsic viscosity ranging from 0.33 to 0.54 dl g^{-1} was obtained. The measured value decreases with the increasing of soft segment content due to the less rigid characteristic of polyetheramide (i.e. soft segment) components.

2.2. Equipment and experiments

DSC experiments were carried out in a Perkin–Elmer DSC 7. The temperature and the heat flow scales were then carefully calibrated using standard materials. The sample size was more than 10 mg for all the studies. The samples were first heated to 295 °C, T_{max}, which is about 15 °C above the equilibrium melting temperature of PET homopolymer ($T_m = 280$ °C) [32] in order to eliminate the crystalline residues formed during the preparation procedure of samples. For polyether–polyester having 50 wt% soft segment content, the T_{max} is 250 °C. The polymer samples were then either quenched at a rate of 150 °C min^{-1} to room temperature to generate amorphous glassy samples or rapidly cooled to a preset temperature for isothermal crystallization. The crystallization time was about 10 times of exothermic peak time to complete crystallization. The value of peak time was determined by exothermic process of isothermal crystallization. The temperature

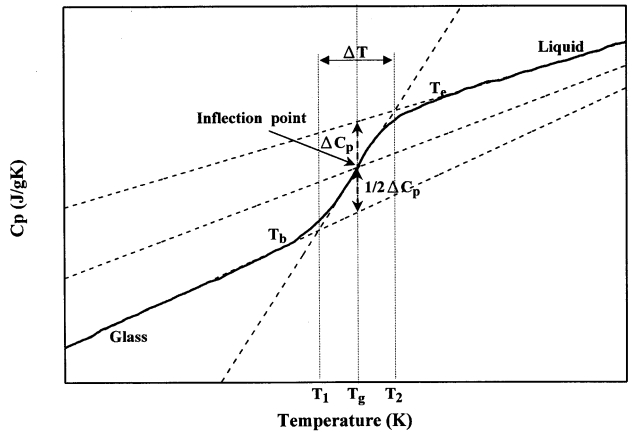

Fig. 2. Temperature dependence of heat capacity in the range of glass transition.

dependence of heat capacity for polymer samples was thus determined according to the execution of blank, calibration and sample runs based on the standard procedure described in the textbook of thermal analysis by Wunderlich [32]. A heating rate of 10 °C min^{-1} was used for all the measurements. Thermal degradation after high temperature treatment may lead to significant changes in melting behavior. In order to alleviate the problem, the testing sample having high annealing temperature was used only once each time for DSC measurements. No evidence of severe degradation problem was found in DSC analysis. Detailed descriptions with respect to the degradation problem of the polyether–polyesters have been addressed in our previous report [16].

On the basis of thermodynamics, the glass transition is defined as an apparent second-order transition [32]. The glass transition is specified as the temperature at which the heat capacity is midway between the liquid and glassy states. In other words, the temperature should be the half-vitrification of the liquid state, and is usually determined as the midpoint of the changes in heat capacity between the liquid and glassy states. The glass transition temperature is thus obtained from the intersection of the mid-value line of two linear dependent lines of heat capacity and the transition curve of heat capacity as shown in Fig. 2. However, the temperature dependence of heat capacity is not always linear. It is possible to exhibit a non-linear increase before or after the transition as the cases of crystallized polyether–polyesters in this study. An alternative is to find the point of inflection in the heat capacity. It has been shown that this midpoint temperature usually corresponds closely to the point of inflection. As examined for pure PET and amorphous polyether–polyesters in this study, the difference between the temperatures of intersection point and inflection point is less than 1 °C. For the sake of systematic studies, the glass transition temperatures of this study are measured as the inflection point of the heat capacity in the range of glass transition.

Thin films of bulk polyether–polyester samples having thickness of micrometer range and of 10s of nanometer for PLM and TEM observations, respectively, were obtained by ultra cryomicrotomy using a Reichert Ultracut microtome (equipped with a Reichert FCS cryochamber and a diamond knife). All the samples prepared by cryomicrotomy were operated at −120 °C. PLM image was obtained by an OLYMPUS BX60 PLM installed with a DP10 digital camera. Staining was accomplished by exposure the samples to the vapor of a 2% aqueous OsO_4 solution for overnight. Bright field TEM images were obtained by the mass-thickness contrast on a JEOL JEM-1200 × TEM, at an accelerating voltage of 120 kV. The sample of the amorphous part appeared relatively dark after staining by OsO_4, while the sample of the crystallized part appeared light. For comparison, solvent-cast samples were also prepared for morphological observations. The polyether–polyester thin films were prepared by casting a 0.1–1% (w/w) polyether–polyester and 1,1,2,2-tetrachloroethane solution onto carbon-coated glass slides. The samples were then crystallized at different crystallization temperatures from the melt. The thermal treatments were similar to the microsectioned samples. The crystallized samples were then shadowed by Pt and coated with carbon again. After shadowing, the films were stripped and floated onto the water surface and then recovered using copper grids.

For WAXD experiments, the same crystallization conditions as described in Section 1 were carried out on homopolymer and copolymer bulk samples. A Siemens D5000 1.2 kW tube X-ray generator (Cu Kα radiation) with a diffractometer was used for WAXD powder experiments. The scanning 2θ angle ranged between 5 and 40° with a step scanning of 0.05° for 3 s. The diffraction peak positions and widths observed from WAXD experiments were carefully calibrated with silicon crystals with known crystal size.

3. Results and discussion

3.1. Compatibility studies in polyether–polyesters

The compatibility between polyetheramide (soft) and polyester (hard) segments was studied by differential scanning calorimetry. The polyether–polyesters were quenched from the melt to −120 °C, about 50 °C below the glass transition temperature (T_g) of polyetheramide, ED2003 ($T_g \sim -69$ °C). No indication of crystallization during quench was identified in terms of DSC measurements and PLM observations. There are no exothermic peaks observed during rapid cooling (−150 °C min^{-1}) in DSC measurements. No crystalline birefringence is found by PLM observations at ambient temperature for the quenched samples. Only one glass transition was found in DSC thermograms during heating after the polyether–polyesters were quenched into liquid nitrogen. Polyetheramide and

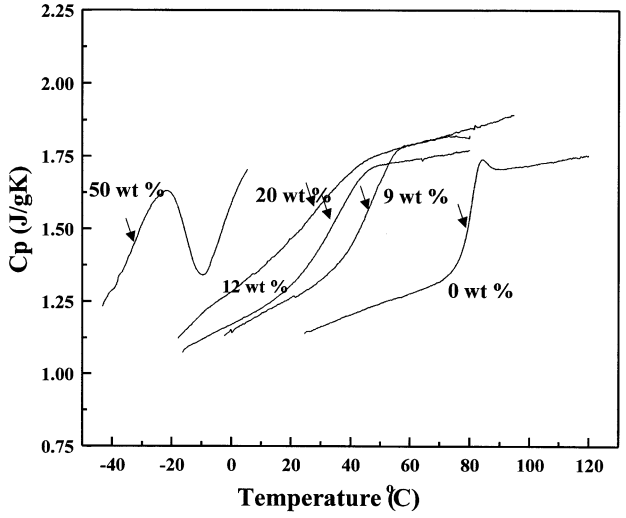

Fig. 3. Temperature dependence of heat capacity for polyether–polyesters having: (a) 0, (b) 9, (c) 12, (d) 20, (e) 50 wt% soft segment contents.

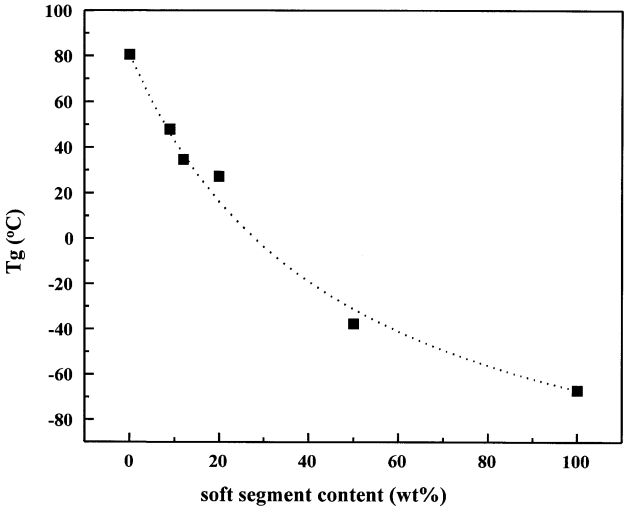

Fig. 4. Composition dependence of glass transition temperatures for polyether–polyesters. The dashed line was calculated from Eq. (1).

polyester segments become compatible in the melt after copolymerization. Large degree (above sub-micrometer) phase separation between soft and hard segments does not occur during quench. Furthermore, the glass transition range was found to broaden towards the lower temperature side with increasing the content of soft segment. We suggest that the broadening is the results of transition from the completely miscible state to the partial segregation of polyetheramide component so that a profile of concentration gradient for polyetheramides is formed (see below for reasons). Fig. 3 shows the temperature dependence of heat capacity for the polyether–polyesters having different soft segment contents. The T_g of amorphous copolymer gradually decreases with increasing soft polyetheramide segment content. It is noted that an exothermic peak for the polyether–polyester having 50 wt% soft segment content was observed in Fig. 3. The exothermic response is the result of soft polyetheramide segment crystallization.

The composition dependence of T_g of the polyether–polyesters is shown in Fig. 4. The dashed line in Fig. 4 are derived using the theoretical equation [21]

$$\ln T_g = \frac{W_1 \Delta C_{p1} \ln T_{g1} + W_2 \Delta C_{p2} \ln T_{g2}}{W_1 \Delta C_{p1} + W_2 \Delta C_{p2}} \quad (1)$$

where W_1 and W_2 are the weight fractions of the components, ΔC_{p1} and ΔC_{p2} are the heat capacity increments at T_g, and T_{g1} and T_{g2} are the transition temperatures of the pure constituents. The equation was derived from the mixed system entropy of two miscible polymers based on thermodynamic arguments, assuming temperature-independent heat capacity increments. The values of T_{g1} and ΔC_{p1} for pure PET are determined from Fig. 3 as 353.7 K and 0.368 J g^{-1} K, respectively. The values of T_{g2} and ΔC_{p2} for pure polyether are obtained from literature as 206 K and 0.870 J g^{-1} K [32]. It is evident that the predicted composition-dependent T_g corresponds well with the experimental results. On the basis of thermodynamic origin, we simply modified the system molar entropy for the segmented copolymers as

$$S = X_1 S_1 + X_2 S_2 + \Delta S_p \quad (2)$$

The pure component entropies per unit mass are denoted as S_1 and S_2 and their respective weight fractions as X_1 and X_2. The ΔS_p represents the excess entropy including all contributions arising from copolymerization. Following the similar derivation for the prediction of composition-dependent T_g by Couchman [21], the same relation as Eq. (1) can be obtained as described in following. At the glass transition, the system entropy exhibits a characteristic of transition continuity. The continuity thus gives the composition relations as

$$X_1 \left\{ \int_{T_{g1}}^{T_g} \left(C_{p1}^{g} - C_{p1}^{l} \right) \mathrm{d} \ln T \right\} + X_2 \left\{ \int_{T_{g2}}^{T_g} \left(C_{p2}^{g} - C_{p2}^{l} \right) d \ln T \right\} + \Delta S_p^{g} - \Delta S_p^{l} = 0 \quad (3)$$

where the superscript g and l indicates the glass and the melt states, respectively. Eq. (1) is obtained by assuming temperature-independent heat capacity increments as long as the ΔS_p terms in glassy state (ΔS_p^{g}) and in the melt (ΔS_p^{l}) are either both trivial or equal to each other. The connectivity in copolymer segments formed by copolymerization inevitably makes a profound effect on the excess entropy. The agreement between theoretical and experimental results in the polyether–polyesters explicitly reflects that ΔS_p also exhibits an analogous continuity at transition.

Provided the significant effect of segment connectivity on ΔS_p, there are many factors such as specific interactions, non-random segment distribution as well as non-combinatorial

term to affect ΔS_p. These contributions on ΔS_p render the problem of excess entropy for copolymers much more complex than the compatible blend systems. The differences between ΔS_p^g and ΔS_p^l might be varied on copolymer constituents and their constituted chemical structure as well as compositions. In other words, the temperature dependence of T_g for polyether–polyesters shall be found more or less departure from that of an ideal or regular solution from which Eq. (1) is achieved. Nevertheless, if the experimental results agree with the predicted dependence described by Eq. (1), the examined system can be viewed as a miscible pair of constituents. As a result, this correspondence suggests that the forced miscibility of soft and hard segments in copolymer approaches the segmental level, and copolymerization indeed provides compatibilized effect to intrinsically incompatible constituents. Furthermore, we speculate that the copolymerization effect on ΔS_p of the polyether–polyesters offset all the contributions on ΔS_p and thus, nullify the effect of ΔS_p on system entropy. The mixing effect on system entropy of copolymer is thus balanced by the penalty of chain connectivity.

3.2. Segregation of non-crystallizable soft segments in copolymers

To investigate the crystallization behavior of polyether–polyesters, samples of polyether–polyesters after various thermal treatments were sectioned by cryo-microtomeand and then, examined by PLM and TEM. The focus of this morphological study is to explore the segregation behavior of polyetheramide segment during the crystallization of polyester component. As reported in our previous studies for the polyether–polyesters having a low content of the soft segment (soft segment content is below 15 wt%) [16], no significant texture and contrast for phase separation was observed for staining amorphous samples under TEM. Similar results for amorphous polyether–polyesters having soft segment content up to 50 wt% was observed in this study. No evidence of microscopic segregation (above a several nanometer length scale) for polyetheramide component was found.

Contrary to the observations of amorphous samples, it was observed that typical spherulites with negative birefringence grow radially and finally, impinge against each other for crystallized samples while the soft segment content is less than 20 wt% (see figs. 5–7 in Ref. [16]). However, distinct PLM textures were observed as soft segment content equal to or above 20 wt%. As an example shown in Fig. 5(a) (20 wt% soft segment content), crystallized polyesters form crystalline domains but loss of the negative birefringence of spherulites. Corresponding TEM results, as shown in Fig. 5(b), indicate that the lamellar aggregates of polyester component form less organized crystalline fibrils but still fully cover the whole sample area. Much perceptible textures were obtained from solvent-cast samples as shown in Fig. 6. Two segregation processes for the amorphous segments in crystallizable copolymers and blends during crystallization have been proposed by Cheng and Wunderlich [33]. These two processes are microscopic segregation between the crystallized lamellae and macroscopic segregation among the spherulites. This observed morphology suggests that no sign of macroscopic segregation (above sub-micrometer length scale) for polyetheramide component can be observed after the crystallization of polyester. The crystallizable polyester segments grow to form lamellae with amorphous portions embedded in the region between neighboring lamellae due to the connectivity between the low molecular weight polyetheramide and polyester segments. The specific texture is similar to the observations of the growth of baby spherulites in polyethyleneoxide (PEO) reported by Cheng and coworkers [34]. A schematic illustration of the crystallized polyether–polyesters is thus proposed as shown in Fig. 7. Solid line and dashed line denotes polyester hard segment and polyetheramide soft segment, respectively. This illustration is a combination of proposed morphologies by

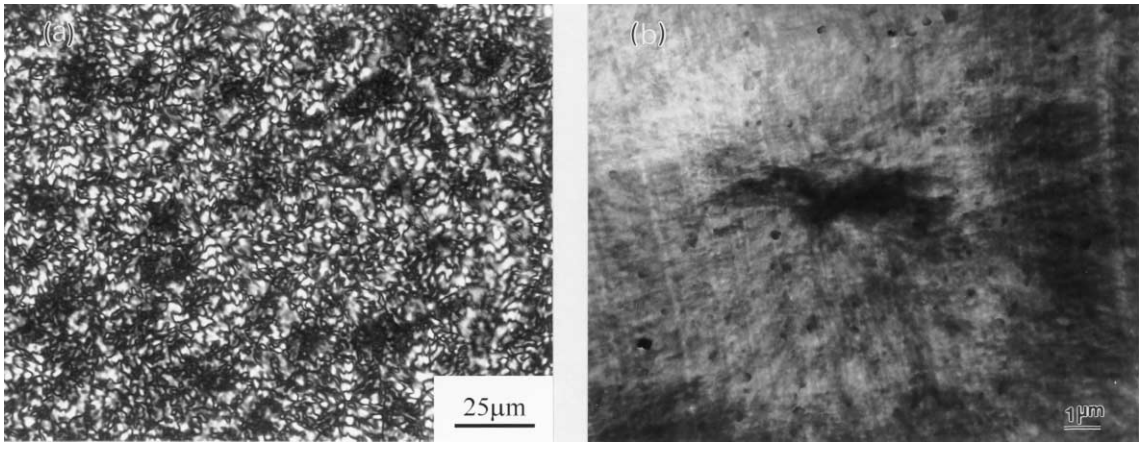

Fig. 5. (a) PLM and (b) TEM micrographs of microsectioned polyether–polyesters containing 20 wt% soft segment content isothermally crystallized at 220 °C from the melt.

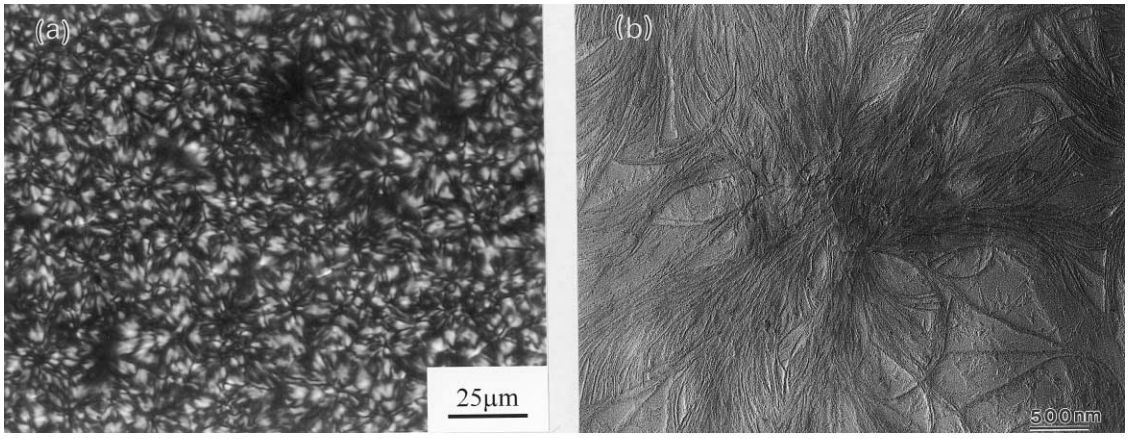

Fig. 6. (a) PLM and (b) TEM micrographs of solvent-cast polyether–polyesters containing 20 wt% soft segment content isothermally crystallized at 220 °C from the melt.

Cella [4] and Seymour et al. [6]. Similar morphological textures have been found while soft segment content is less that 40 wt%. Further increasing the soft segment content, the segregation of the soft segments is found among the spherulites of crystallized hard segments as shown in Fig. 8. In other words, the crystallized polyester spherulites are isolated by the formation of amorphous domains. It is of interest to recognize that two types of segregation appear for these crystallizable copolymers. We suggest that the formation of these textures is attributed to the behavior of exclusion model crystallization (see below for reasons).

3.3. Exclusion model in crystallization

As proposed for the crystalline morphology of polyether–polyesters, the non-crystallizable soft component certainly affects the crystallization behavior of polyester segments. The soft segment may reside as defects within polyester crystals, or it may be excluded from the crystals to form amorphous segregation. In other words, crystal structures may be constructed in two different ordering processes. Crystallizable segments may co-crystallize different segments to form co-crystals or crystals with defected components, or to exclude out the alien segments to form crystal structure of their own. The first instance is so-called the inclusion model and the latter instance is the exclusion model for the crystallization of dissimilar chains [35]. For the size of soft segment, the latter should be most likely the consequence. Fig. 9 shows the WAXD results of pure PET and crystallized polyether–polyesters having 12 wt% soft segment content. For pure PET, unit cell parameters of $a = 0.481$ nm, $b = 0.571$ nm, $c = 1.083$ nm, $\alpha = 96.7°$, $\beta = 128.1°$, $\gamma = 107.2°$ were approximately calculated by least-squares refinement based on the specific plane spacing [36]. In contrast to PET, the structure parameters of the examined copolymer were calculated as $a = 0.493$ nm, $b = 0.590$ nm, $c = 1.086$ nm, $\alpha = 97.7°$, $\beta = 127.6°$, $\gamma = 107.6°$. The dimension of chain-axis and the geometry of structural unit (i.e. the axial angles) of polyester crystals determined from the WAXD patterns are little variant. The introduction of soft segments to polyether–polyesters only slightly increases the dimensions of chain packing for polyester crystals. The cell volumes of the pure PET and the copolymer are 2.051 and 2.163 nm^3, respectively. This result reflects that the structural dimensions of crystalline polyester segments in copolymers are not significantly disturbed by the presence of polyetheramide component. Similar results were also obtained for different polyether–polyesters.

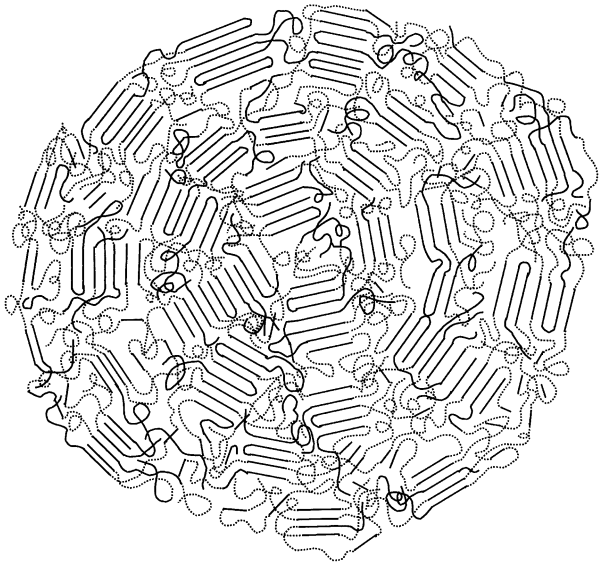

Fig. 7. Schematic diagram of the morphology of crystallized polyether–polyesters. Solid line and dashed line denotes polyester hard segment and polyetheramide soft segment, respectively.

To further explore the mechanism, a series of T_g measurements for crystallized polyether–polyesters at different crystallization stages (i.e. different crystallinity) was performed. The polyether–polyesters were isothermally crystallized at different crystallization temperatures from the melt, and then quenched to −120 °C for DSC heating

experiments. Usually, the glass transition temperature of semi-rigid homopolymer such as PET increases with increasing the so-called rigid-amorphous fraction, first proposed by Cheng and co-workers [37], due to the constrain effect of polymer chain at crystal-amorphous interface. Similar results have been observed in this study as shown in Fig. 10(a). The T_g of PET increases with increasing the isothermal crystallization temperature due to the increase of the rigid-amorphous fraction of PET. In contrast to the pure PET, an opposite result was found for the T_g change of polyether–polyesters. The glass transition of polyether–polyesters decreases with the crystallization time as shown in Fig. 10(b)–(d). Similar results have been found in all of the polyether–polyesters studied at different crystallization temperatures besides the sample having 50 wt% soft segment content. This observation in T_g change with respect to crystallization provides the evidence to visualize the behavior of polyether–polyester chains during crystallization. The change of T_g during crystallization (Fig. 10) suggests that the polyetheramide component is excluded from the polyester crystals during crystallization. The exclusion of the polyetheramide soft segments from polyester crystals leads to the composition changes of amorphous regions. The increase of soft segment content in the amorphous regions thus decreases the T_g of amorphous components since the polyester hard segments are continuously used up. The results of T_g variation with crystallization time are consistent with the morphological observations. Also, the heat capacity of crystallized polyether–polyesters exhibits a different transition behavior as compared to that of pure PET. For pure PET, the transition range, defined as the temperature difference between the temperatures of T_1 and T_2, is almost invariant for samples at different crystallization stages (Fig. 11). In contrast to pure PET, the glass transition range for the polyether–polyesters gradually broadens corresponding to the crystallization time and mainly extends to the low temperature side of transition as shown in Fig. 12. Besides the decrease in T_g, the broadening gives rise to a change in the shape of the temperature dependence of heat capacity. A non-linear increase of the heat capacity of the liquid state up to the vicinity of glass transition temperature was observed as shown in Fig. 12(e). On the basis of thermal analysis and

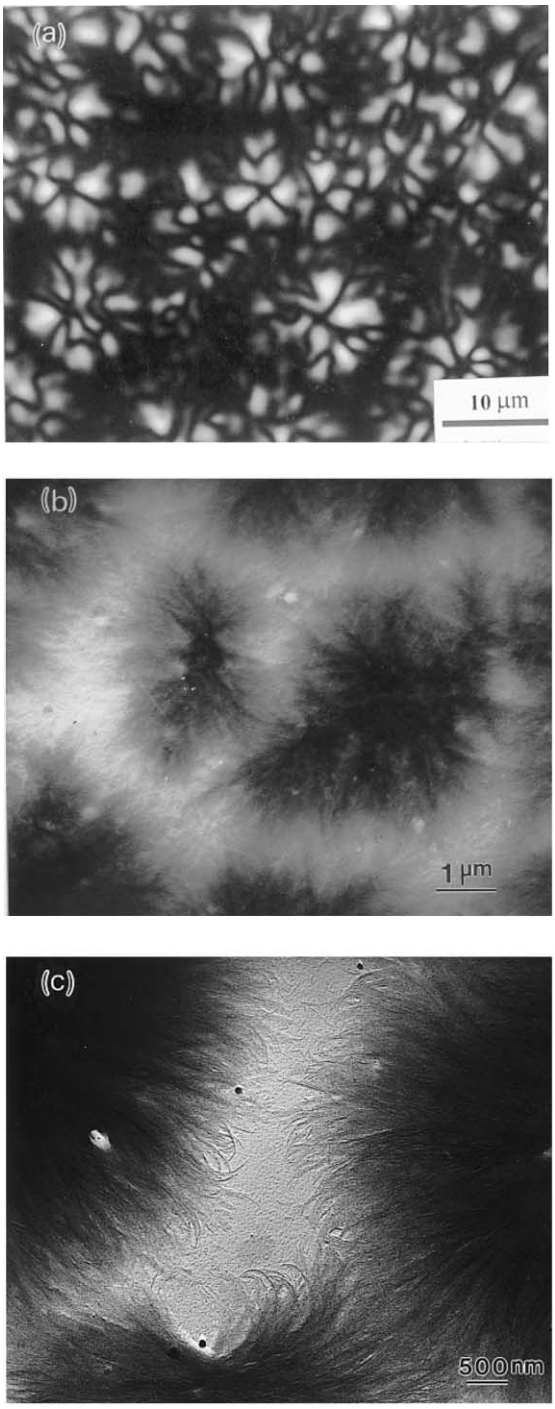

Fig. 8. (a) PLM and (b) TEM micrographs of solvent-cast polyether–polyesters containing 50 wt% soft segment content isothermally crystallized at 160 °C from the melt, (c) the enlarged area of inter-spherulites in TEM micrograph.

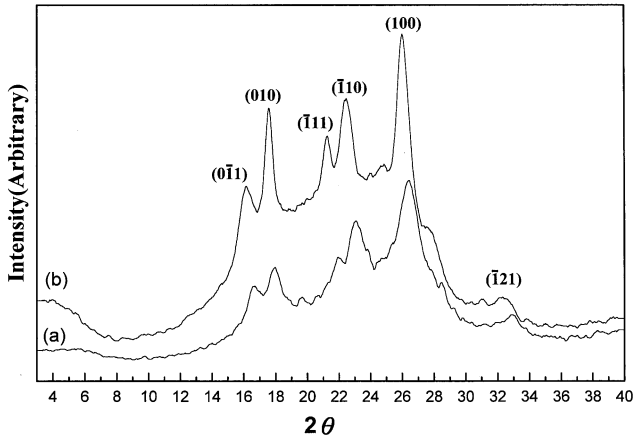

Fig. 9. WAXD powder patterns of: (a) pure polyester and (b) polyether–polyesters containing 12 wt% soft segment contents both crystallized at 190 °C. The assignment of diffraction peaks was based on the works of Liu and Geil [32].

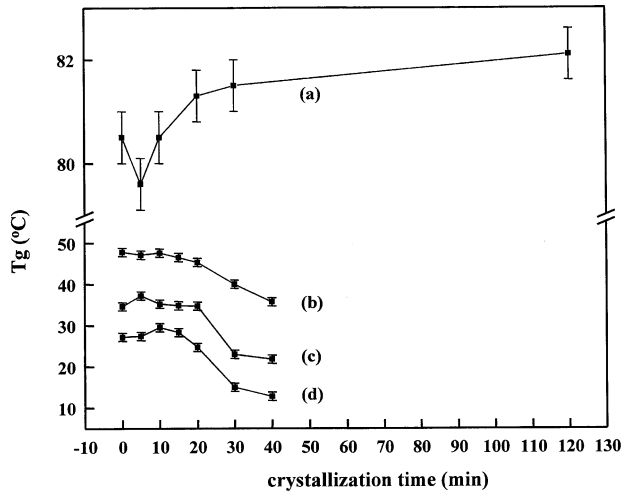

Fig. 10. Effect of crystallization time on glass transition temperatures for polyether–polyesters containing: (a) 0, (b) 9, (c) 12, and (d) 20 wt% soft segment contents. The isothermal crystallization temperatures for above samples are 210, 200, 190 and 220 °C, respectively.

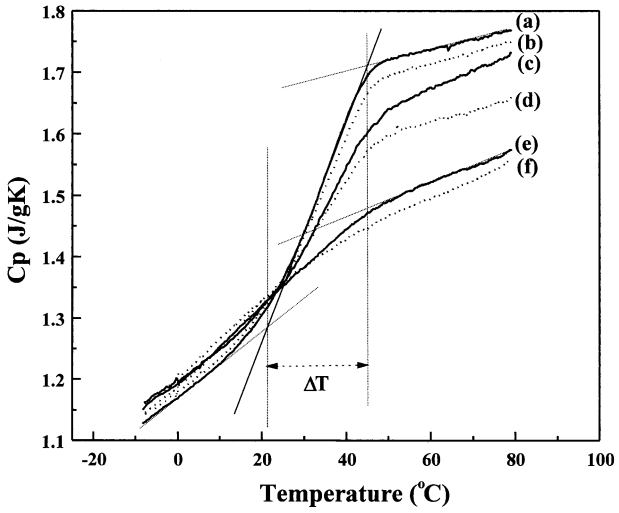

Fig. 12. Temperature dependence of heat capacity for: (a) amorphous polyether–polyester containing 12 wt% soft segment content and the polyether–polyester crystallized at 190 °C for different crystallization times: (b) 10, (c) 15, (d) 20, (e) 30, (f) 40 min.

morphological observations, we suggest that the observed transition behavior for crystallized polyether–polyesters is attributed to the characteristic of exclusion process. In the progress of the exclusion of polyetheramide segments from the polyester crystals, the soft segments in amorphous portions gradually construct a concentration profile. Fig. 13 illustrates the idealized schematic diagram of the concentration profile for polyetheramide component after crystallization. This is a typical behavior of excluded amorphous segments between neighboring lamellae. Further increasing the content of soft segment, the continuous growth of polyester spherulites is inhibited due to the shortage of polyester segments. As a result, the impingement of polyester spherulites has not been observed as shown in Fig. 8 (50 wt% soft segment content). The exclusion of soft segments thus form partial segregation between the polyester lamellae as well as among the polyester spherulites. In fact, it is very unusual to form macroscopic segregation among spherulites if the polyether–polyester is truly a multiple block copolymer of that there is connectivity between polyetheramide and polyester segments. We hypothesize that the copolymerization of polyetheramide and polyester segments is not

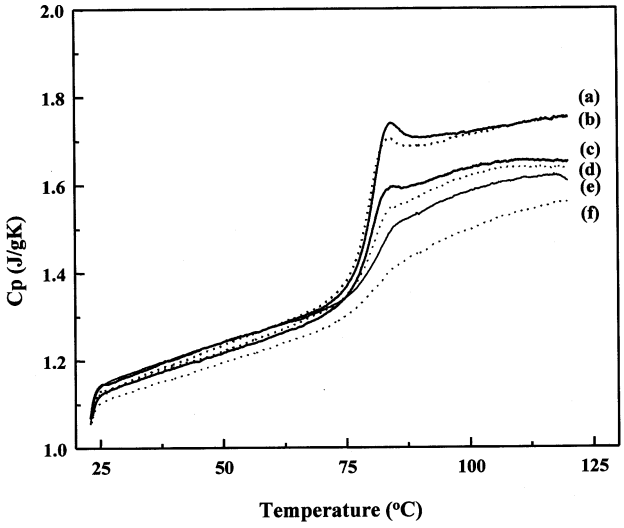

Fig. 11. Temperature dependence of heat capacity for: (a) amorphous PET homopolymer and PET crystallized at 210 °C for different crystallization times: (b) 5, (c) 10, (d) 20, (e) 30, (f) 120 min.

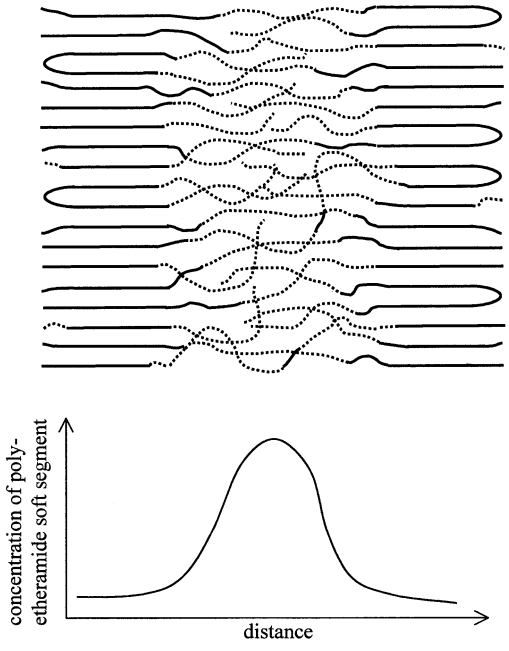

Fig. 13. Idealized schematic diagram of concentration gradient profile of the soft segment for crystallized polyether–polyesters. Solid line and dashed line denotes polyester hard segment and polyetheramide soft segment, respectively.

homogeneously carried out. According to the synthetic route, it is highly possible to form the polyetheramide having broadening molecular weight distribution, in particular, the copolymers containing high content of polyetheramide. In other words, there may exist high molecular weight of polyetheramide as evidenced by the appearance of polyetheramide crystallinity (for instance, the polyether–polyester containing 50 wt% soft segment content) so that the macroscopic segregation may occur. Further experiments with respect to the chemical structure and the crystallization behavior of the crystalline–crystalline polyether–polyesters are currently carried out in our laboratory.

4. Conclusions

The forced compatibility of polyetheramide and polyester segments in their block copolymers was studied in terms of thermal analysis and morphological observations. The polyetheramide component was miscible with polyester component after copolymerization as evidenced by the observations of single glass transition and of homogeneous texture. The T_g of polyether–polyesters decreases with increasing soft segment content. A theoretical prediction of composition-dependent glass transition exhibits consistent results with the experimental observations. This correspondence suggests that the mixing effect on system entropy of copolymer is balanced by the penalty of chain connectivity. Based on the decrease of T_g in the progress of isothermal crystallization, an exclusion model for the crystallization of polyester segments in copolymers was proposed. Furthermore, the corresponding broadening towards the low temperature side in the glass transition reflects the formation of concentration gradient profile in the amorphous regions. It is of interest that two types of soft segment segregation, between polyester lamellae and among polyester spherulites, were also observed in this study.

Acknowledgements

The financial support of the National Science Council (Grant NSC 89-2216-E-005 -023) is acknowledged. The authors would like to thank Dr Stephen Z.D. Cheng at Maurice Morton Institute of Polymer Science of University of Akron for his helpful discussion. R.M.H. would like to thank Ms S.-Y. Lee of Regional Instruments Center at NSYSU and Ms P.-C. Chao of Regional Instruments Center at NCHU for their help in the WAXD and the ED experiments, respectively.

References

[1] Legge NR, Holden G, Schroeder HE. Thermoplastic elastomers, a comprehensive review. California: Academic Press, 1987.
[2] Brown M, Witsieppe WK. Rubber Age 1972;104:35.
[3] Hoeschele GK, Witsieppe WK. Angew Makromol Chem 1973;29:267.
[4] Cella RJ. J Polym Sci, Polym Symp 1973;42:727.
[5] Shen M, Mehra U, Niinomi M, Koberstein JT, Cooper SL. J Appl Phys 1974;45:4182.
[6] Seymour RW, Overton JR, Corley LS. Macromolecules 1975;8:331.
[7] Lilaonitkul A, West JR, Cooper SL. J Macromol Sci Phys 1976;2:563.
[8] Hoeschele GK. Angew Makromol Chem 1977;58:299.
[9] Wegner G, Fujii T, Meyer W, Lieser G. Angew Makromol Chem 1978;74:295.
[10] Lilaonitkul A, West JR, Cooper SL. Macromolecules 1979;12:1146.
[11] Zhum LL, Wegner G. Makromol Chem 1981;182:3625.
[12] Vallance MA, Cooper SL. Macromolecules 1984;17:1208.
[13] Miller JA, Lin SB, Hwang KKS, Wu KS, Gibson PE, Cooper SL. Macromolecules 1985;18:32.
[14] Miller JA, McKenna JM, Pruckmayr G, Epperson JE, Cooper SL. Macromolecules 1985;8:1727.
[15] Sheen YC, Lin JJ. Submitted for publication.
[16] Ho RM, Hseih PY, Yang CC, Lin JJ. J Polym Sci, Polym Phys Ed, in press.
[17] Cohen RE, Cheng PL, Douzinas K, Kofinas P, Berney CV. Macromolecules 1990;23:324.
[18] Nojima S, Kato K, Yamamoto S, Ashida T. Macromolecules 1992;25:2237.
[19] Gordon JM, Rouse GB, Gibbs JH, Risen Jr WM. J Chem Phys 1977;66:4971.
[20] Couchman PR, Karasz FE. Macromolecules 1978;11:117.
[21] Couchman PR. Macromolecules 1978;11:1156.
[22] Seguela R, Prud'homme J. Polymer 1989;30:1446.
[23] Cohen RE, Cheng PL, Douzinas K, Kofinas P, Berney CV. Macromolecules 1990;23:324.
[24] Nojima S, Kato K, Yamamoto S, Ashida T. Macromolecules 1992;25:2237.
[25] Cohen RE, Bellare A, Drzewinski MA. Macromolecules 1994;27:2321.
[26] Rangarajan P, Register RA, Adamson DH, Fetters LJ, Bras W, Naylor S. Macromolecules 1995;28:1422.
[27] Ryan AJ, Hamley IW, Bras W, Bates FS. Macromolecules 1995;28:3860.
[28] Hamley IW, Fairclough JPA, Terrill NJ, Ryan AJ, Lipic PM, Bates FS. Macromolecules 1996;29:8835.
[29] Zhu L, Chen Y, Zhang A, Calhoun BH, Chun M, Quirk RP, Cheng SZD, Hsiao BS, Yeh F, Hashimoto T. Phys Rev B 1999;60:10,022.
[30] Kimura M, Porter RS, Salee GJ. Polym Sci, Polym Phys Ed 1983;21:367.
[31] Hoeschele GK. Die Angew Makromol Chem 1977;58:299.
[32] Wunderlich B. Thermal analysis. California: Academic Press, 1990.
[33] Cheng SZD, Wunderlich B. J Polym Sci, Polym Phys Ed 1986;24:577 see also p. 595.
[34] Cheng SZD, Barley JS, von Meerwall ED. J Polym Sci, Polym Phys Ed 1991;29:515.
[35] Cheng SZD, Janimak JJ, Zhang A, Hsieh ET. Polymer 1991;32:648.
[36] Liu J, Geil PH. J Macromol Sci Phys 1997;B36(1):61.
[37] Cheng SZD, Pan R, Wunderlich B. Makromol Chem 1988;189:2443.